VOL. 10, NO. 18, OCTOBER 2015 ISSN 1819-6608
ARPN Journal of Engineering and Applied Sciences

www.arpnjournals.com

COMPRESSIVE FORCES OF CELL INDUCED LONGITUDINAL DEFORMATION TO THE LIQUID CRYSTAL SURFACE

Chin Fhong Soon[1], Kian Sek Tee[2], Mansour Youseffi[3] and Morgan Clive Thomas Denyer[4]
[1]Biosensor and Bioengineering Laboratory, MiNT-SRC, Universiti Tun Hussein Onn Malaysia, Batu Pahat, Johor, Malaysia.
[2]Faculty of Electrical and Electronic Engineering, Universiti Tun Hussein Onn Malaysia, Batu Pahat, Johor, Malaysia.
[3]School of Engineering, Design and Technology-Medical Engineering, University of Bradford, Bradford, United Kingdom.
[4]School of Medical Sciences, University of Bradford, Bradford, United Kingdom.
E-Mail: soon@uthm.edu.my

ABSTRACT

The ability of a cell to contract plays an important role in determining the ability of the cell to migrate, proliferate and associating with other cells. The transduction of the force in soft substrate such as the liquid crystal surface is a method proposed to study the traction forces of single cells. In this work, finite element method was used to study the compressive forces induced by the keratinocyte to the liquid crystal surface via the anchorage of focal contacts. The constitutive finite element model of the liquid crystal-focal contacts was established. The stress and displacement were analyzed using linear static stress analysis for a quiescent cell. The data for lateral displacements obtained from the experiment were provided as inputs to develop the model and verified through the output acquired for both simulation and experiment. The simulation results indicated that the cell compressive stresses were in the range of 14.93 ± 1.9 nN/μm^2 per focal contact. Based on the result obtained, it was suggested to model focal contact-liquid crystal interface with a compressive model that can better approximate the mechanism observed.

Keywords: compressive forces, keratinocyte, deformation, liquid crystal.

INTRODUCTION

Cell traction forces reveal the ability of a cell to contract and regulate the physical functionalities of cells such as adhesion, migration and cytokinesis. Liquid crystals have been applied in detecting single cell forces via the deformation lines induced by the traction forces of cells (Soon *et al.* 2013). The transduction of forces from the cell into deformation lines in the liquid crystal (LC) surface are mainly controlled by the cytoskeleton structures of the cells that are interconnected by sub-components of actin filament, focal adhesions and integrins (Burridge *et al.* 1996; Chin Fhong Soon *et al.* 2014). It was hypothesized that "pinching" forces were exerted by the cells in generating a liquid crystal deformation line which projects obliquely at the periphery of the cell (Chin Fhong Soon *et al.* 2010). Cytochalasin-B, a depolymerization cytochemical, was employed to interrogate the release of forces after the actin filaments were disrupted with this cytochemical (Chin Fhong Soon *et al.* 2010). However, this drug acted generally to the cytoskeletons that are distributed in the encapsulation of cytoplasm. In the quest of the mechanism of the tangential forces applied to the peripheral of the cells, it was assumed that the circumferential actin filament lining at the boundary of the cells play a role in regulating the traction of keratinocytes (Owaribe *et al.* 1981). A study on the deformation profiles of the liquid crystal surface as induced by the focal contacts was implemented based on the linear static analysis. A three dimensional model that represents the liquid crystal and the focal contacts was established to enable the study of the stress model. The model was simulated with an assumption that the liquid crystal has a semi solid sub-phase and hence, strained in bi-directional via a pair of focal contacts of a cell.

MATERIALS AND METHODS

Establish finite element model of the cell focal contacts-liquid crystal

Prior to the simulation of the model proposed in the SolidWorks software, basic parameters such as the physical structures of the focal contacts, properties of the liquid crystals and cell geometry must first be established. The establishment of the model took into considerations of the contractions of the short marginal actin filaments found at the periphery of the cell. The proposed model included a cell model hypothetically placed on the LC slab representing the LC coating having a thickness of 100 μm. The LC coating was assumed to be homogeneously coated and has a height (Hlc), length (Llc) and width (Wlc) of 30 x 100 x 100 μm, respectively as shown in Figure 1a. For the LC model, a restrain plane was assigned to the bottom of the liquid crystal slab representing an immobilized substrate on the petri dish. In the LC model, hollow rectangular structures approximate the focal contact clusters was grafted to the surface of the liquid crystal surface and distributed at the periphery of the cell (Figure 1a). To enable a normal force (F) transversely applied to the focal contact-LC interface, a hollow space was assigned to the rectangular shaped focal contacts and the focal contacts were lodged in the LC surface. The entrenched focal contact cluster or vinculin has a length (Lfa), thickness (Hfa) and width (Wfa) that was assumed containing two or three accumulations of vinculins (Peterson *et al.* 2004). The model and dimensions proposed were based on the measurements results obtained from the immunofluorescence stainings of the vinculins reported previously (Soon *et al.* 2013). Hence, the close

contact plane in which the stress applied was obtained by multiplying Hfa and Lfa.

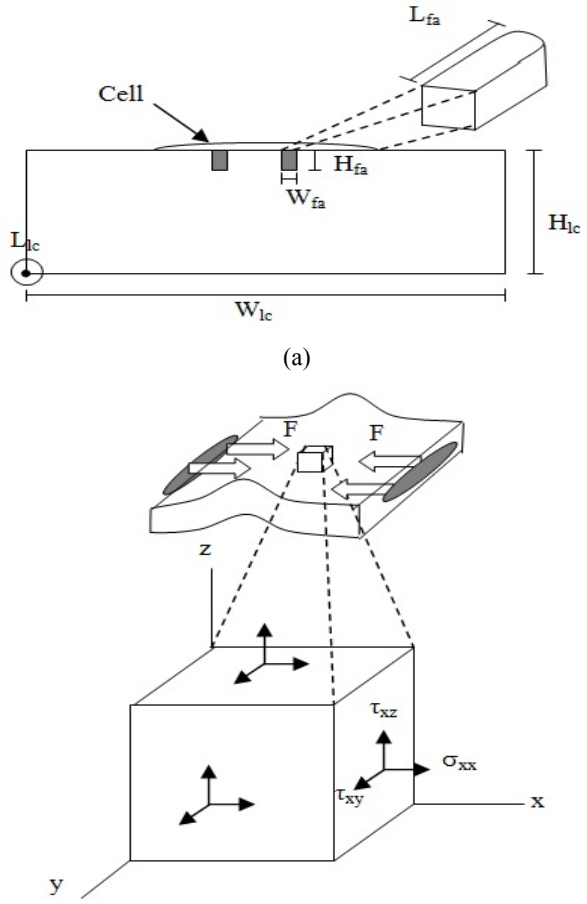

Figure-1. (a) The geometrical information of the focal contacts-liquid crystal model. L_{fa}, H_{fa}, W_{fa}, L_{lc}, H_{lc}, and W_{lc} are the parameters for the length, height and width of the focal contacts (denoted as fa) and the liquid crystal substrate (denoted as lc), respectively. (b) LC surface model under uni-axial compressive force (F) exerted by two cluaster of focal contacts. Bottom: a tensor diagram describing the stresses in three dimensions. The plane stress, σ_{xx} induced shear stress of τ_{xz} and τxy in the y and z directions.

Table-1 summarized the physical properties of the liquid crystal coating and focal contacts applied in the finite element model. For establishing the constitutive model of the stress-strain parameters, a stress tensor diagram (Figure-1b) was used to illustrate the influence of the principal stress in x-plane (σ_{xx}) from the focal contacts and shear stress to the liquid crystal slab in the y and z directions (τ_{xy} and τ_{xz}). The pair of compression stresses applied to the liquid crystal surface in x direction created a resultant LC deformation in y and z directions.

Table-1. Properties of the LC coating and dimension of the Vinculin.

Properties of model	Dimensions
LC coating	Thickness = 100 µm, Width x Length = 50 x 50 µm
Young's modulus	110 kPa
Poisson's ratio	µ = 0.5 (maximum limit configurable in Cosmosworks)
Dimension of vinculin	H_{fa} = 1 µm, W_{fa} = 0.5 - 1 µm, L_{fa} = 1.3 – 2.8 µm

From the cell relaxation experiment as published previously (C. F. Soon *et al.* 2013), transverse displacement (Δx) at the focal contact-liquid crystal interface was obtained. These data were provided to the model established in quantifying the compressive forces using a finite element simulation (Cosmoswork) software. Prior to the application of linear static analysis and computation of stresses, the model was meshed into 10842 of triangular elements. Subsequently, the von-Mises stress of the model was computed. Based on the experiment in which the cell applied stress to the liquid crystal surface within the linear viscoelastic range or well within 10 % of strain, this could induce reversible changes of the liquid crystal (C. F. Soon *et al.* 2011). Hence, the application of von-Mises stress is an indication of the stresses produced without exceeding the yield strength of the material (Donald, 2007). The criterion set for the yield strength of 923.7 nN/□m2 satisfied the model where small forces in nano-newton range were applied. In this model, yield strength of incompressible rubber was specified for the liquid crystals.

The linear static analysis package available in the Cosmosworks/Solidworks based on the finite element method was used to analyze the traction forces applied to the focal contact. The linear static analysis package provides solution to the linear elastic problem based on Hooke's method and the minimum total potential energy method (Fagan, 1992). For the finite element model established, the force matrix {F} is associated with the displacement, {U} via the relationship of {F} = [k]{U}, in which [k] is the stiffness matrix (Fagan, 1992).

In the properties settings of the software, a Young's modulus of 110 kPa and Poisson's ratio of 0.5 was pre-determined for the finite element model in the software. The optimum Poisson's ratio should be 0.58 as determined previously in a micro-tensile experiment (Ching Fhong Soon *et al.* 2011). However, 0.5 is the Poisson's ratio limit which could be set in the software. Due to the incompressibility of the liquid crystal, Poisson's ratio of 0.5 is feasible (Dimitriadis *et al.* 2002). However, both calculation at Poisson's ratio of 0.58 and simulation at Poisson's ratio at 0.5 will be investigated.

RESULTS AND DISCUSSIONS

Five stress sites were implemented to the model of liquid crystals-focal contacts in the Solidworks software as shown in Figure-2. With the simulation limit of the

software the solid model was meshed into 10842 triangular elements having a size of 5.7 µm (Figure-2). The von-Mises stresses and deformation found at the stress site of the liquid crystal are highly correlated with the transverse displacements induced by the cell (Figure-3). In both computation and finite element simulations, the compressive forces simulated have a linear relationship with to the transverse displacements induced by the cell (Figure-4a). However, the simulated stresses induced by the cell at each stress site were presented with small variations (mean ± SD = 14.93 ± 1.9 nN/□m2) indicating that a quiescent cell tend to express balancing forces at the periphery of the cell (Figure-3 and Figure-4b). From the simulation result, it was understood that the cell displayed an iso-diametric characteristic in which this is influenced by the arrangement of the actin filaments and distributions of the lamellipodia spread marginally around a quiescent keratinocyte (Henry *et al.* 2003; Kirfel *et al.* 2004; Owaribe *et al.* 1981).

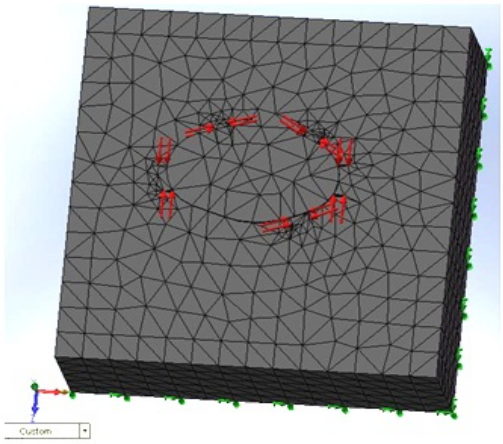

Figure-2. A mesh containing 10842 triangular elements at a size of 5.7 µm was used in generating the solid mesh for the focal contacts-liquid crystal model.

Based on the simulation result in Figure-4a, the forces distributed around the cell were ranged from 25 to 90 nN. This result is in good agreement with the forces of epithelial cells published previously at a range of 5 – 35 nN (Roure *et al.* 2005). The range of forces expressed were lower is due to the different characteristic of cell adhesion substrate in which the cell in the experiment by Roure, 2005 isolated the focal contacts via micro fabricated cantilever instead of focal contacts in large clusters. In a continuous continuum, the adherent cell has the space to anchor focal contacts in groups and hence, enabling them to exert larger forces from the intracellular actin cytoskeletons (Burridge *et al.* 1997; Peterson *et al.* 2004). Larger expression of forces on a continuous surface can also be understood from via an experiment using AFM to probe cervical cells. Sagvolden and co-worker (Sagvolden *et al.* 1999) demonstrated that cervical carcinoma cell requires 100 – 200 nN to dissociate from a glass surface. In addition, the epithelial cells were shown to detach from a surface with an exposure of tangential force at 100 nN in a centrifuge (Thoumine *et al.* 1996). A continuous surface provides larger contact area between the cells and substrate leading to higher adhesion forces. From the simulation, the result indicated that keratinocyte exerted lower force in comparison to the cell adhesion force to the glass substrate. For lowly motile cell such as keratinocyte, the force transmitted to a surface should be relatively lower than highly motile cell such as fibroblast. However, this is yet to be investigated through dynamic simulations of cell forces.

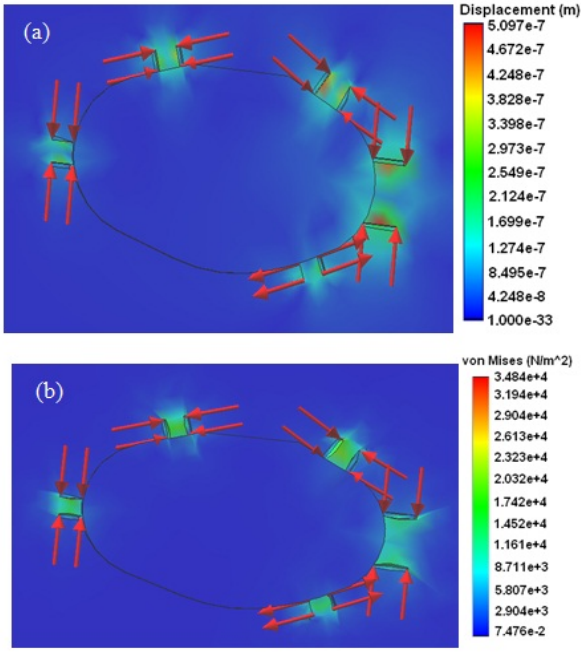

Figure-3. (a) Transverse displacement and (b) von Mises stress analyzed by Finite Element method for the keratinocyte simulated.

A Poisson's ratio of 0.58 for the liquid crystal was used in the calculation while 0.5 was used for the finite element simulation. The value 0.58 was determined from the micro-tensile experiment (Ching Fhong Soon *et al.* 2011). Based on this theory, the finite element model established at a Poisson's ratio of 0.5 was simulated with higher forces compared to the calculated forces at a Poisson's ratio at 0.58. The difference between the simulation and calculation results yielded a 20% difference as indicated in Figure-4 could be due to the slight different of Poisson's ratio used. As a result, the simulated forces were found higher in contrast to the calculated forces due to the lower Poisson's ratio applied to the simulation model. Usually, stiffer material has a lower Poisson's ratio. To achieve same displacement of material, a stiff material (lower Poisson's ratio) required higher forces to be deformed than a soft material (higher Poisson's ratio).

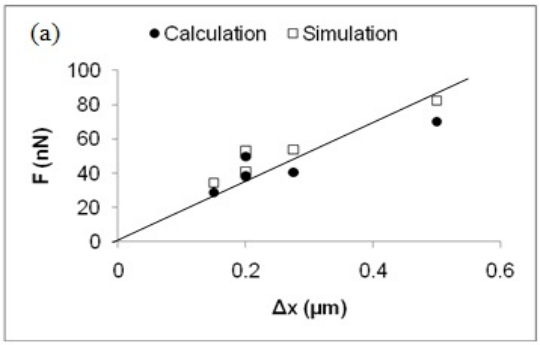

(a)

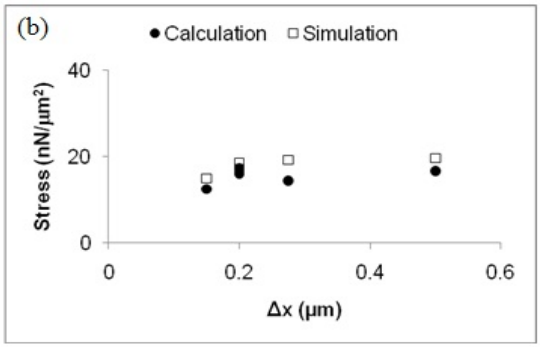

(b)

Figure-4. The relationship between the (a) applied force to the displacements and (b) von-Mises stress to the displacement, both by calculation and simulation.

Figure-5 shows the simulation details of the stress distribution at a stress site. Two similar focal contacts with an area of 4.2 μm^2 were formed in contact with the liquid crystal surface. At the contact area, identical compressive forces were applied to each stress plane in the normal plane. In Figure 5, the maximum lateral displacement at approximately 0.5 μm was induced by lateral force per stress plane at F = 82.36 nN. The correlated stress to this displacement is 34.84 $nN/\mu m^2$ (Figure-5b). At the stress exertion location, highest nodal stress and transverse displacement were identified right at the two stress planes where the interface was located. Both stresses and displacements decreased quadratically from the stress planes to the central region of the deformation site (Figure-6).

In the simulation, the profiles of the stress and displacement found at the deformation site seemed to be in good agreement with the contraction pattern observed in experiments. Both results via experiment and simulation indicate that the deformations are in close association with the compression and shears of the contact material. These mechanisms were probably related to the traction forces applied due to the contraction of the circumferential action filaments via the focal contacts. Simultaneous contraction of the short action filaments around the cell created forces that drove the contact area closer to each other or a decrease in the width of the deformation line. This mechanism is better known as pinching. Hence, the result indicates that compression model is suggested to be used to describe the mechanism of a sedentary cell contracting on the LC surface.

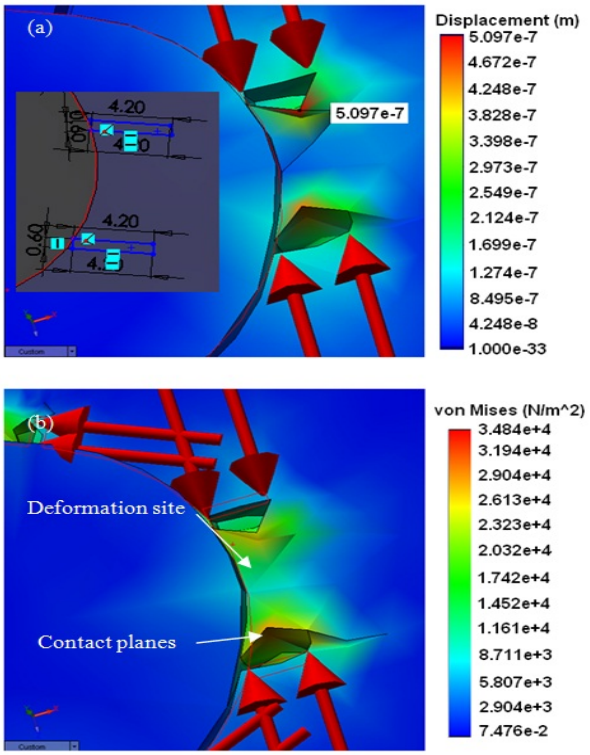

Figure-5. (a) A 3-D simulation of a deformation with loads applied to the focal contact planes and LC surface. Inset: The dimensions of the focal contacts used in the finite element model. (b) Von-mises stresses computed for the compressive loads.

The deformation lines formed in the LC surface as a result of the contraction of cell were modeled using a bi-axial strains as applied at the interface (C. F. Soon *et al.* 2013). It is important to note that that the longitudinal deformation in the LC formed was a secondary effect related by the Poisson's ratio of the LC. This was attributed to the trajectory of the pairs of shear forces which was induced by the focal contacts. Focal contacts are a group of macromolecules proteins that are linked to the actin filaments. Any polymerization of the actin filaments or contractions would create pulling forces to the focal contacts. An experiment involved with cytochalasin-B treatment to the cell could reveal the effect of relaxed actin filaments in releasing the transverse strains and longitudinal deformations of the LC (C. F. Soon *et al.* 2013). Cytochalasin-B is a cytochemical that is specific in depolymerization of the actin proteins which in turn relieved the stress exerted to the focal contacts. However, it is uncertain whether this model is suitable for a larger stress planes and higher stresses. Some parameters such as the vinculin size, deformations and displacements required to be verified experimentally.

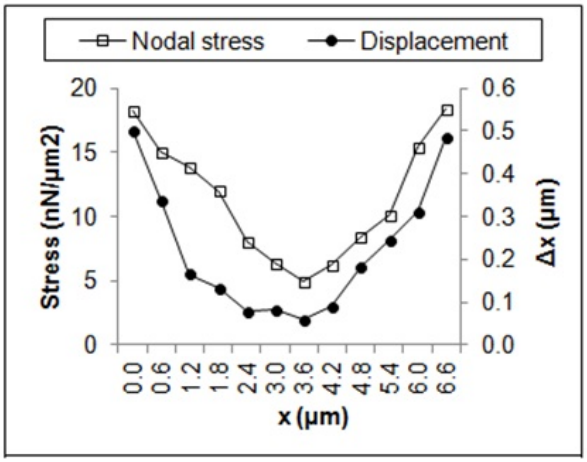

Figure-6. The distribution of stresses and transverse displacements across a deformation site.

CONCLUSIONS

Linear static analysis of the liquid crystal-focal contacts interface revealed that the forces applied to form longitudinal deformation are compressive in nature. Lateral displacement at the stress site is correlated with the normal faces applied to the contact area. The displacement in both y and z direction is linearly proportional to the stress applied within the 10% strain of the liquid crystal. The variation of loaded forces is well within a few nano-newtons even though focal contacts may vary in sizes. This suggests that the driving forces could also be contributed by the intracellular actin filaments. At the deformation site, the highest stresses and displacement were found at the initial location of the focal contacts. Nonetheless, the model presented is in good agreement with the observation in previous experiments.

ACKNOWLEDGEMENTS

The authors are grateful to the research financial support Science Fund Vot S024/Project No. 02-01-13-SF0104 awarded by Malaysia Ministry of Education (MOE).

REFERENCES

[1] Burridge K., Chrzanowska-Wodenicka M. and Zhong C. 1997. Focal adhesion assembly. Trends in Cell Biology Vol. 7, pp. 342-347.

[2] Burridge K. and Chrzanowska-Wodnicka M. 1996. Focal adhesions, contractility and signaling. Annual Review of Cell and Developmental Biology, Vol. 12, pp. 463-519.

[3] Dimitriadis E. K., Horkay F., Maresca J., Kachar B., and Chadwick R. S. 2002. Determination of elastic moduli of thin layers of soft material using the atomic force microscope. Biophysical Journal, Vol. 82, pp. 2798-2810.

[4] Donald B. J. M. 2007. Practical stress analysis with finite elements. Dublin: Glasnevin publishing.

[5] Fagan M. J. 1992. Finite element analysis: theory and practice. Singapore: Longman.

[6] Henry G., Li W., Garner W. and Woodley D. T. 2003. Migration of human keratinocytes in plasma and serum and wound re-epithelialisation Lancet, 361, pp. 574-576.

[7] Kirfel G. and Herzog H. 2004. Migration of epidermal keratinocytes: mechanisms, regulation, and biological significance. Protoplasma, Vol. 223, pp. 67-78.

[8] Owaribe K. Kodama R. and Eguchi G. 1981. Demonstration of contractility of circumferential actin bundles and its morphogenetic significance in pigmented epithelium in vitro and in vivo. The Journal of Cell Biology, Vol. 90, pp. 507-514.

[9] Peterson L. J., Rajfur Z., Maddox A. S., Freel C. D. Chen Y., Edlund M. 2004. Simultaneous stretching and contraction of stress fibers in vivo. Molecular Biology of the Cell, Vol. 15, pp. 3497-3508.

[10] Roure O. D., Saez A., Buguin A., Robert H. A., Chavrier P., Siberzan P. 2005. Force mapping in epithelial cell migration. Proceedings of the National Academy Sciences of the United States of America, Vol. 102, No. 7, pp. 2390-2395.

[11] Sagvolden G., Giaever I., Pettersen E. O. and Feder J. 1999. Cell adhesion force microscopy. Proceedings of the National Academy Sciences of the United States of America, Vol. 96, pp. 471-476.

[12] Soon C. F., Wan Omar W. I., F. Berends R., Nayan N., Basri H., Tee K. S. 2014. Biophysical characteristics of cells cultured on cholesteryl ester liquid crystals. Micron, Vol. 56, pp. 73-79.

[13] Soon C. F., Youseffi M., Berends R. F., Blagden N. and Denyer M. C. T. 2013. Development of a novel liquid crystal based cell traction force transducer system. Biosensors & Bioelectronics, Vol. 39, pp. 14-20.

[14] Soon C. F., Youseffi M., Blagden N. and Denyer M. 2010. Effects of an enzyme, depolymerization and polymerization drugs to cells adhesion and contraction on lyotropic liquid crystals. Proceedings of the World Congress on Engineering Vol. 1, pp. 556-561.

[15] Soon C. F., Youseffi M., Blagden N. and Denyer M. 2011. Influence of time dependent factors to the phases and Poisson's ratio of cholesteryl ester liquid

crystals. Journal of Science and Technology Vol. 3, No. 1, pp. 1-20.

[16] Soon C. F., Youseffi M., Gough T., Blagden N. and Denyer M. C. T. 2011. Rheological characterization of the time-dependent cholesteric based liquid crystals and in-situ verification. Materials Science and Engineering C, Vol. 31, No. 7, pp. 1389-1397.

[17] Thoumine O., Ott A. and Louvard D. 1996. Critical centrifugal forces induce adhesion rupture or structural reorganization in cultured cells. Cell Motility and the Cytoskeleton Vol. 33, pp. 276-287.